geoconvention
Calgary • Canada • May 15-19 2017

Finite-difference simulation of microseismic events associated with hydraulic-fracturing stimulation: Case study in a CBM reservoir

Germán Rodríguez-Pradilla[a] *and David W. Eaton*[a]

[a] *Department of Geoscience, University of Calgary.*

Summary

The finite-difference method is considered the most reliable numeric solution for the partial differential equations that define seismic waves. It is capable to predict the complex behavior of elastic seismic waves in a heterogeneous media like the Coalbed-Methane (CBM) reservoir analyzed in this case study. The simulated propagation of seismic waves are compared with real seismic waveforms of high signal-to-noise-ratio microseismic events recorded with surface seismic stations for earth model calibration, and are extremely useful for a further robust processing of surface microseismic data that includes a fast 3D hypocenter location method and the Moment Tensor Inversion (MTI) of the same microseismic events for an accurate seismic source characterization.

Introduction

The CBM reservoir analyzed in this case study is located close to the northern limit of Cesar-Rancheria Basin, in Colombia. The reservoir of interest is in the Cerrejón Formation from the lower Paleogene period, and is composed by coal beds interbedded by calcareous sandstones (Rodríguez-Pradilla, 2015). At the study area, the Cerrejón formation is covered by quaternary alluvial deposits mainly composed by sands and conglomerates over 600 meters thick. Three vertical wells were drilled to evaluate the production of methane gas from the coal beds (Wells A, B, and C, in Figure 1). For Well A, sonic, density, and gamma ray logs were acquired between 80 and 1020 meters depth, covering most of the Cerrejón formation and the overburden quaternary deposits. And for Well B, a dipole sonic log was acquired between 550 and 1460 meters deep. This log doesn`t cover the quaternary deposits needed to perform a finite difference modeling for surface stations, but has a well-defined linear relation between P and S wave velocities that was used to calculate the S-Wave velocity log of Well A from its P-wave velocity log, obtaining a full initial earth model for Well A composed by P and S wave velocities and density logs (see Figure 3a).

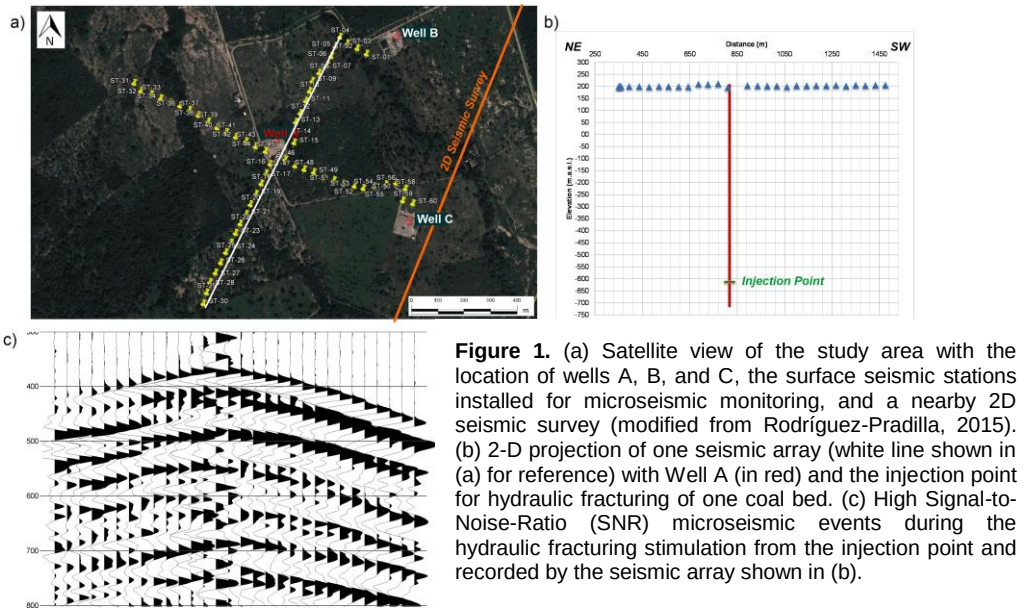

Figure 1. (a) Satellite view of the study area with the location of wells A, B, and C, the surface seismic stations installed for microseismic monitoring, and a nearby 2D seismic survey (modified from Rodríguez-Pradilla, 2015). (b) 2-D projection of one seismic array (white line shown in (a) for reference) with Well A (in red) and the injection point for hydraulic fracturing of one coal bed. (c) High Signal-to-Noise-Ratio (SNR) microseismic events during the hydraulic fracturing stimulation from the injection point and recorded by the seismic array shown in (b).

Large amounts of methane gas can be stored in coal beds as adsorbed gas due to coal's large internal surface area. According to the Theory of Langmuir, a fast dewatering process is required to reduce the formation pore pressure and release the adsorbed methane gas for production (Anderson & Simpson, 2003). This fast dewatering process depends on the coal permeability, which is mostly driven by its natural fractures (or cleats). However, under greater depths (and thus high overburden stress), the

cleats are closed reducing the permeability to the range of milliDarcys (Nuccio, 2000). This makes necessary a hydraulic fracturing treatment on for the coal beds of interest to increase their permeability, and therefore its methane gas production capacity. For Well A, a multistage hydraulic fracturing was defined for several coal beds between 700 and 1000 meters deep. Coal beds can be easily identified in density logs due to its low bulk density (around 1.3 g/cc) compared with the interbedding lithologies (above 2.0 g/cc), as shown in Figure 2. Some stages of this hydraulic fracturing treatment were monitored using wireless surface seismic stations with 1-component 10-Hz vertical geophones (Figure 1). The seismic waveforms recorded with this surface array during the hydraulic fracturing of one 8-meters thick coal bed at 825 meters below the ground surface were used for the 2-D finite difference modeling discussed in this manuscript.

Fracability Analysis of Coal Beds

A common velocity model calibration procedure consists on the identification of calibration shots in the seismic data and a further adjustment for traveltimes and sensor orientation (Maxwell, 2014). However, for the hydraulic fracturing stimulation in the CBM reservoir, the well casing was drilled for each stage using a jetting technique consisting on the injection of water and sand slurry at high pressure to wear the steel casing. This technique doesn't generate a clear seismic signal (as a conventional perforation shot does). Therefore, no clear calibration shots were available for this study, and an additional fracability analysis of the stimulated coal beds was performed to estimate a depth location of the detected microseismic events.

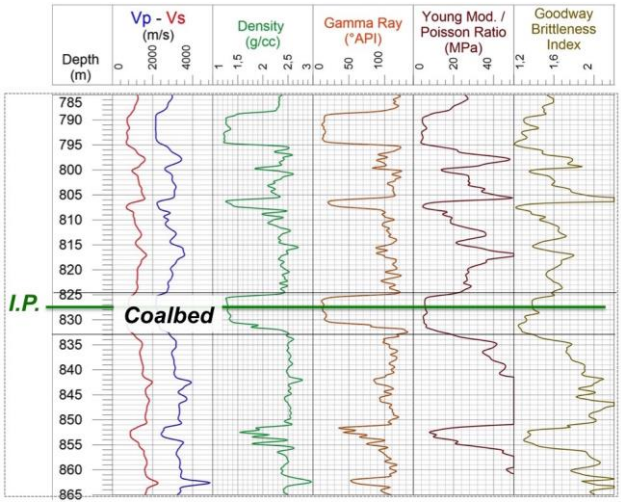

Figure 2. Dipole sonic, density, and Gamma Ray logs, and the calculated fracability logs from Well B, showing the stimulated coal bed and the Injection Point.

The elastic modulus of the coal beds and the interbedding lithologies were calculated from the dipole sonic and density logs of Well B following the seismic velocity equations for isotropic media (Mavko, Mukerji, & Dvorkin, 2009), and two fracability parameters were calculated (See Figure 2). The first one correspond to the ratio between Young Modulus to Poisson's Ratio, and the second one is the Goodway Brittleness Index ($BI_{Goodway}=(\lambda+2\mu)/\lambda$). Both fracability parameters show similar contrast between the coal beds and the interbedding lithologies. This contrast, together with the presence of natural fractures (or cleats) in the coal beds, suggest that the fractures generated by the hydraulic fracturing stimulation should be geomechanically constrained to the stimulated coal beds. This depth constraining assumption is implemented for the further finite-difference modeling and velocity model calibration by determining that the hypocenter of the registered microseismic event shown in Figure 1c is located at the same depth than the injection point of the hydraulic fracturing treatment. This depth assumption is later assessed in this manuscript following a RMS residual error optimization method for hypocenter location.

The Finite Difference Method

The Finite Difference algorithm implemented was originally developed by (Boyd, 2006) as a Matlab script, and optimized for the 2D simulation of microseismic events. An explosive source at the inection point was implemented together with absorbing boundary condition, as developed by Hidgon (1991), to prevent unwanted waves reflections from the grid boundaries. A preliminary earth model is obtained by applying a lowpass filter to the sonic and density logs from Well A (Figure 3a). For this earth model, multiple reflections and deformations are shown during the simulation (Figure 3b) caused by the highly vertical variation of the seismic velocities and density profiles due to the presence of the coal beds. The vertical displacements obtained for the surface seismic stations (Figure 3c) show a clear P-phase first arrival followed by multiple reflections, resembling the same phenomena observed on the recorded microseismic events shown in Figure 1c. Once the input parameters are defined for a 2D Finite-Difference simulation of the case study

(grid spacing, source location and mechanism), an optimum earth model must be calculated for subsequent processing of the acquired surface microseismic data, like hypocenter location and fault-plane solution. This earth model (as shown in Figure 3a) is composed by P-Wave and S-Wave velocity, and a density profiles. A first approach to obtain these profiles is the sonic and density well logs recorded on Well A where the hydraulic-fracturing treatment was performed. The S-Wave log for this well was computed from a linear regression function obtained from the dipole sonic log of Well B.

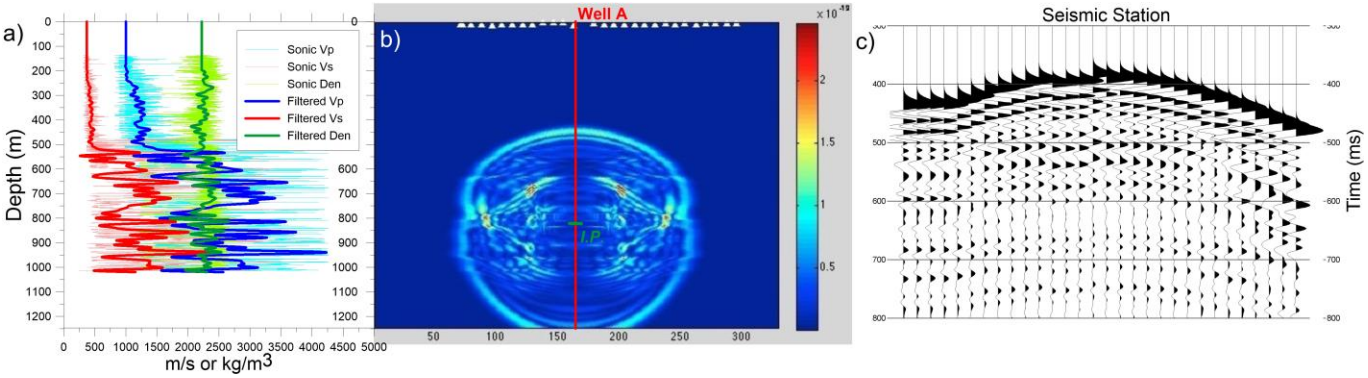

Figure 3. 2D Finite-Difference modeling for the CBM reservoir. (a) Initial earth model (filtered P and S seismic velocities, and density profiles –solid lines- obtained from the dipol sonic and density logs from Well A –pale lines-) used for the simulation. (b) Wave fronts generated by Finite-Difference simulation with the surface seismic stations (in white) and the seismic source located at the injection point of the hydraulic fracturing treatment (in green). (c) Vertical displacement obtained for the surface seismic stations from the Finite-Difference Simulation for the earth model.

The well logs of Well A, shown in "pale" colors in Figure 4a, must be appropriately smoothed before implementing them for a Finite-Difference simulation. This smoothing process was based on the frequency spectrum (Figure 4b) of the high Signal-To-Noise-Ratio (SNR) microseismic event recorded with the surface array (Figure 1c), where an amplitude reduction of the seismic signal is clearly visible for frequencies higher than 100 Hz. Therefore, the velocities and density profiles used to simulate similar waveforms generated by microseismic events shouldn't contain frequencies higher than 100 Hz. To eliminate the non-wanted higher frequencies from the well logs, a depth-to-time conversion was applied with the average P-wave velocity of the sonic log. Then, a Butterworth low-pass filter was implemented with damping frequencies of 100-150 Hz. Finally, a reverse time-to-depth conversion was applied to the filtered profiles using the same P-wave velocity used for the initial conversion. The obtained filtered velocities and density profiles are shown in "strong" colors in Figure 3a, and used for finite-difference simulation.

The P-wave velocity profile was gradually increased to generate synthetic waveforms by finite-difference simulation. The S-wave velocity profile was also subsequently increased by calculating the S-Wave velocity correction from the P-wave correction and the Vp/Vs ratio calculated from the dipole sonic log of Well B. The density profile was not altered for this correction. For each simulated waveforms from the increased P and S wave profiles, the first-breaks were picked and compared to the ones picked in the high SNR microseismic event recorded with the surface array (Figure 1) that is being used as a calibration shot (see Figure 4-c). The difference of traveltimes for each surface seismic station between the picked (real) and calculated (synthetic) traveltimes of the P-phase corresponds to the residual error for each station. The Root-Mean-Square residual error (or RMS error) can be calculated for each velocity profile from the residual error for each station. Figure 4-d shows the obtained RMS errors obtained for different

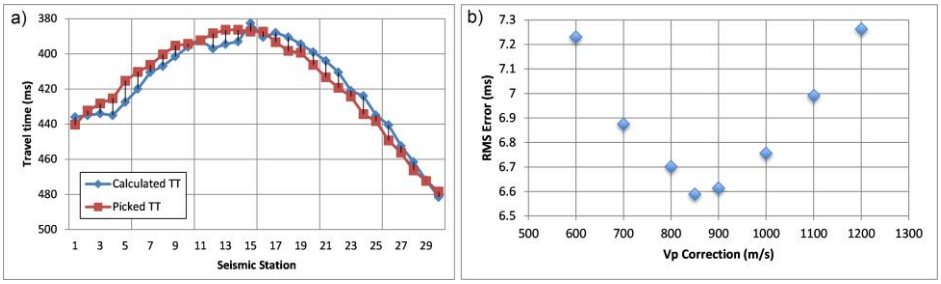

Figure 4. Velocity model calibration for the CBM Reservoir from sonic and density logs, and 2D Finite-Difference modeling. (a) Picked First-Breaks for the P-wave of the high SNR event shown in Figure 1c, and of the simulated wave record shown in Figure 3c. The difference between the two first breaks of each station (black lines) is used to calculate the RMS error of the Finite-Difference simulation. (b) RMS error calculated for different corrections of the P-wave velocity profile, where an optimum correction of 850 m/s is obtained.

corrections for the P-wave velocity profile (and the calculated correction for the S-wave velocity profile), where an optimum correction (i.e. a minimum RMS error) of 850 m/s for the P-wave profile is obtained. This optimum correction is included into the earth model implemented for the hypocenter location of microseismic events associated with the monitored hydraulic-fracturing treatment.

2D Hypocenter Location

A grid-search method can be easily implemented for hypocenter location of microseismic events, once the first-break traveltimes are picked in the real data (i.e. in the high SNR microseismic event shown in Figure 1c) and the velocity model is appropriately calibrated. This grid search method consists on a preliminary calculation of traveltimes from different hypocenters, and a further calculation of the RMS error between the picked and the calculated traveltimes for each hypocenter. The optimal hypocenter solution is the one with the lowest calculated RMS error (Havskov & Ottemöller, 2010).

Figure 5 shows the obtained results of the grid-search method implemented to calculate thy hypocenter location of the high SNR microseismic event used for the velocity model calibration. A first 1-D grid search for different horizontal distances from the injection point and a constant depth was implemented (Figure 5a), where an optimal hypocenter location (i.e. a minimum RMS error) is obtained to be at 30 meters from the injection point. This method was replicated for different depths of the 1-D grid search to obtain a 2-D RMS error profile (Figure 5b), showing a very similar RMS response for all the computed depths. A 1-D section of the 2-D RMS error profile obtained for the optimum hypocenter distance from Figure 5a is shown in Figure 5c, where no optimum hypocenter depth is obtained and leaving a high depth uncertainty of microseismic events' hypocenters typical for surface arrays.

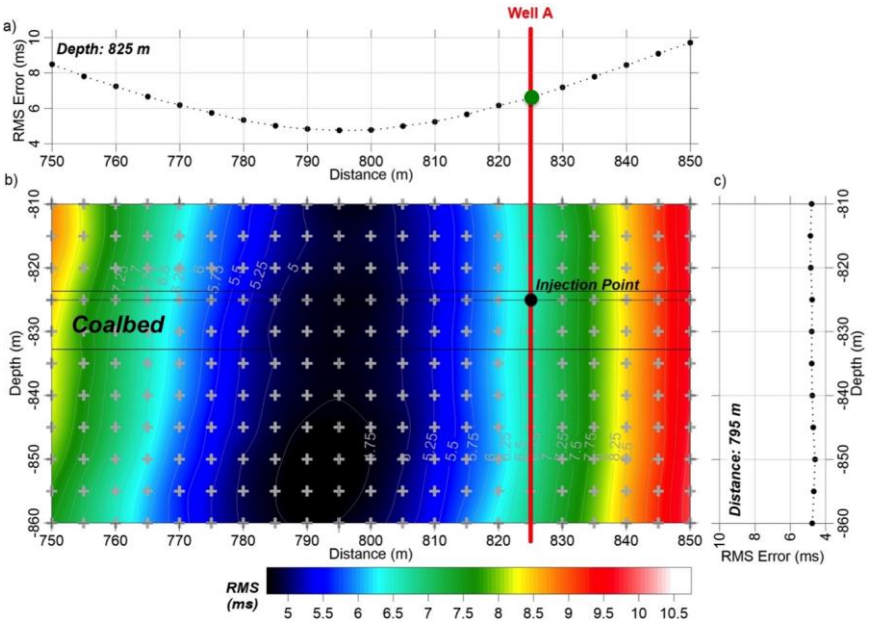

Figure 5. (a) RMS error computed for different hypocenter locations at the depth of the injection point for the hydraulic fracturing treatment (825 meters), showing a clear optimum location at a distance of 795 meters (30 meters from the injection point). (b) 2-D RMS error profile computed for different distances and depths from the injection point. (c) 1-D section of the 2-D RMS error profile for the optimum hypocenter distance obtained in Figure 6a (795 meters), where no optimum hypocenter depth is obtained.

Conclusions

2-D Finite Difference method was used to simulate a microseismic event in a CMB reservoir recorded with surface stations. A further calibration of the earth model derived from sonic and density logs was done by a RMS residual error reduction, obtaining an optimum earth model that was then implemented for a 2D hypocenter location, obtaining an optimum horizontal hypocenter location, but no optimum depth hypocenter location. The synthetic waveforms obtained for the 2-D finite difference modeling and the calibrated earth model resembles the multiple arrivals shown in the real seismic waveforms acquired with the surface monitoring array, and can be implemented for 3-D finite difference simulation applicable for 3-D hypocenter location and Moment Tensor Inversion of detected microseismic events.

Acknowledgements

We gratefully thank the Sponsors of the Microseismic Industry Consortium for their support of this work. GMAS Laboratory and Drummond Ltd. Colombia are also deeply thanked for their support during seismic data acquisition.

References

Anderson, J., & Simpson, M. (2003). Production of Natural Gas from Coal. *Oilfield Review* , 8-31.

Bai, M. (2016). Why are brittleness and fracability not equivalent in designing hydraulic fracturing in tight shale gas reservoirs. *Petroleum* , 1-19.

Boyd, O. S. (2006). An efficient Matlab script to calculate heterogeneous anisotropically elastic wave propagation in three dimensions. *Computers & Geosciences , 32*, 259–264.

Havskov, J., & Ottemöller, L. (2010). *Routine Data Processing in Earthquake Seismology.* Springer.

Hidgon, R. (1991). Absorbing boundary conditions for elastic waves. *Geophysics , 56* (2), 231-241.

Nuccio, V. (2000). Coal-Bed Methane: Potential and Concerns. *USGS Fact Sheet FS–123–00* , 1-2.

Maxwell, S. (2014). *Microseismic Imaging of Hydraulic Fracturing: Improved Engineering of Unconventional Shale Reservoirs.* Society of Exploration Geophysicists.

Mavko, G., Mukerji, T., & Dvorkin, J. (2009). *The Rock Physics Handbook* (Second Edition ed.). Cambridge University Press.

Rodríguez-Pradilla, G. (2015, 08). Microseismic monitoring of a hydraulic-fracturing operation in a CBM reservoir: Case study in the Cerrejón Formation, Cesar-Ranchería Basin, Colombia. *The Leading Edge* , 896-902.